JOURNAL OF MATERIALS SCIENCE 37 (2002) 3615–3622

Oxidation bonding of porous silicon carbide ceramics

J. H. SHE
Synergy Materials Research Center, AIST, Nagoya 463-8687, Japan
E-mail: jihong-she@aist.go.jp

Z. Y. DENG
Synergy Ceramics Laboratory, FCRA, Nagoya 463-8687, Japan

J. DANIEL-DONI, T. OHJI
Synergy Materials Research Center, AIST, Nagoya 463-8687, Japan

A oxidation-bonding technique was successfully developed to fabricate porous SiC ceramics using the powder mixtures of SiC, Al_2O_3 and C. The oxidation-bonding behavior, mechanical strength, open porosity and pore-size distribution were investigated as a function of Al_2O_3 content as well as graphite particle size and volume fraction. The pore size and porosity were observed to be strongly dependent on graphite particle size and volume fraction. In contrast, the degree of SiC oxidation was not significantly affected by graphite particle size and volume fraction. In addition, it was found that the fracture strength of oxidation-bonded SiC ceramics at a given porosity decreases with the pore size but increases with the neck size. Due to the enhancement of neck growth by the additions of Al_2O_3, a high strength of 39.6 MPa was achieved at a porosity of 36.4%. Moreover, such a porous ceramic exhibited an excellent oxidation resistance and a high Weibull modulus.

1. Introduction

Recently, there has been an increasing interest in the use of porous ceramics for hot gas filtration in diesel exhaust systems or in the coal-gasification-generation process in order to limit the emission of some corrosive or toxic particles into the environment. For such applications, the ceramic filters must be able not only to resist the chemical attack at high temperatures by a variety of gases such as O_2, HCl, H_2S, Cl_2, SO_2, NO and H_2O, but also to withstand the mechanical stress or thermal shock in the pulse cleaning process [1, 2]. Due to an unique combination of low thermal-expansion coefficient and good thermal-shock resistance as well as excellent mechanical and chemical stability at elevated temperatures, porous SiC-based ceramics have been considered as one of the most favorable candidates and thus have been extensively tested at different demonstration plants in Europe [3], Japan [4] and USA [5, 6]. The tests have shown some promising results. For example, a clay-bonded SiC filter has been successfully operated at temperatures of 620–845°C in an oxidizing atmosphere for 5855 h [6]. Since the softening temperature of siliceous glassy phases becomes significantly lower in the presence of Na_2O, K_2O and Fe_2O_3, however, clay-bonded SiC filters may be irreversibly elongated and even damaged during long-term operation at higher temperatures [7]. It is expected that such a problem would not arise for self-bonded SiC ceramics. Unfortunately, sub-micron powders and high temperatures are required for production. Moreover, oxidation remains another problem for high-temperature operations of self-bonded SiC filters in an oxidizing atmosphere.

The objective of this work is to develop a low-temperature fabrication technique of porous SiC-based ceramics with superior resistance to oxidation. The approach is schematically illustrated in Fig. 1. The key feature of the process is that SiC powder compacts are heated in air instead of an inert atmosphere. Due to the occurrence of surface oxidation at the heating stage, SiC particles could be bonded each other by the oxidation-derived SiO_2 glass, which may crystallize to cristobalite at temperatures above 1300°C [8, 9]. This technique is referred to as oxidation bonding. As a gas filter, however, a high porosity with a desired pore size distribution is required to achieve a high particulate filtration efficiency and a good gas flow capability. This can be easily realized through the oxidation-bonding process with the incorporation of sawdust, starch, graphite or organic particulates, as illustrated in Fig. 1b. During heat-treatment, these particulates burn out, leaving stable voids in the oxidation-bonded SiC (OBSC) ceramics. This allows the preparation of porous OBSC ceramics with controlled amount, size, shape and distribution of pores. It has been demonstrated [10, 11] that the overall performance of porous ceramics are related not only to the volume fraction and geometrical nature of the pores but also to the size and type of the inter-particle

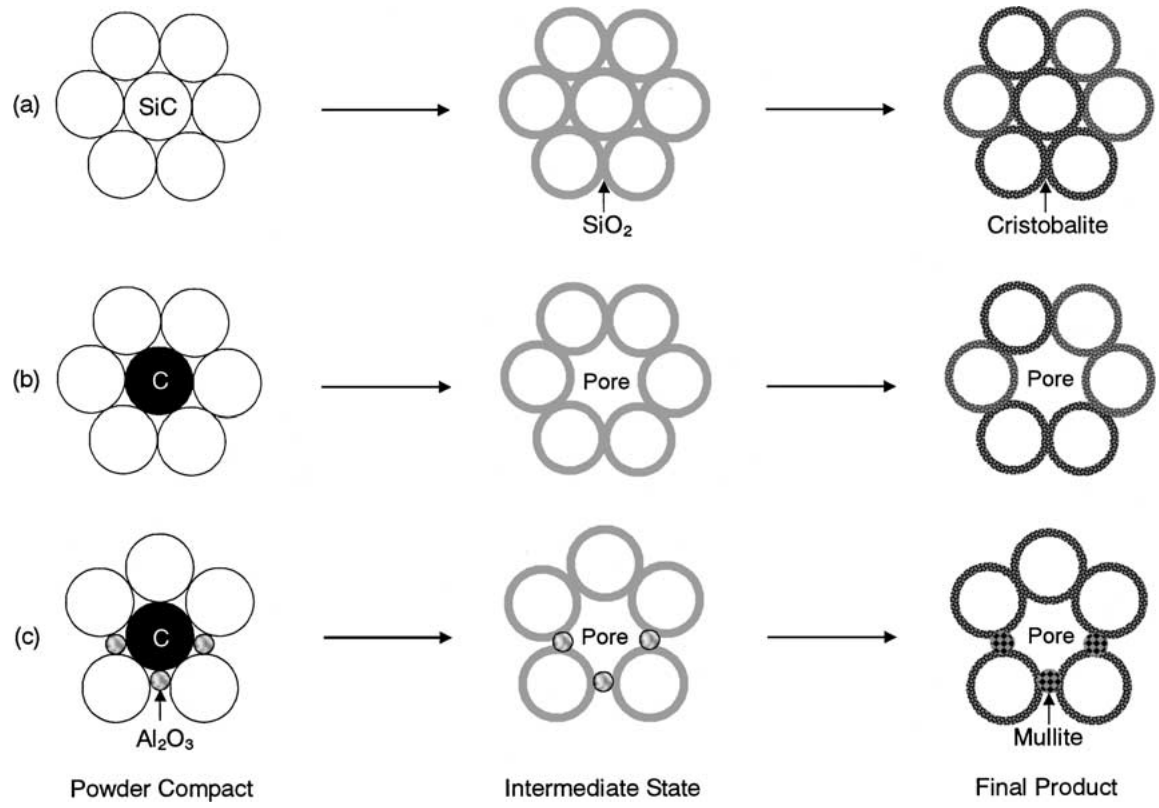

Figure 1 Schematic illustration of (a) undoped, (b) C-doped, and (c) C- and Al_2O_3-doped OBSC process.

connections. In the OBSC ceramics, SiC particles are connected by the amorphous and/or crystalline SiO_2 "bridges". As illustrated in Fig. 1c, the mechanical properties of the SiO_2 bridges and consequently the OBSC ceramics are expected to be improved if some fine Al_2O_3 powders are added, because SiO_2 may react with Al_2O_3 at temperatures over 1400°C to form mullite ($3Al_2O_3 \cdot 2SiO_2$) [12, 13], which has a better mechanical behavior than SiO_2 at both room and elevated temperatures.

In the present work, graphite powders were selected as the pore-forming agent. The oxidation-bonding characteristics, mechanical strength and microstructure of porous OBSC ceramics were investigated as a function of heat-treatment conditions and Al_2O_3 additions as well as graphite particle size and volume fraction.

2. Experimental procedure

A commercially available α-SiC powder (99.7% purity, DU A-3, Showa Denko Co., Japan) was used as the starting material. As can be seen in Fig. 2, the particle morphology is irregular and the size distribution is non-uniform. By a centrifugal photo-sedimentation technique, the mean particle size was determined to be ~2.3 μm, with such a distribution that 34% particles were smaller than 1.0 μm but 33% particles were larger than 5.0 μm and 17% particles were in excess of 10.0 μm. To produce porous SiC ceramics with different pore sizes, three types of graphite powders (99.9% purity, Kojundo Chemical Laboratory Corp., Japan), which had an average particle size of 5.0, 10.0 and 20.0 μm, were employed as the pore-forming agents. Moreover, a submicron α-Al_2O_3 powder (99.99% purity, TM-DAR, Taimei Chemical Co., Japan) was added to improve the mechanical properties. The volume ratio of C, Al_2O_3 and SiC in the initial powder composition was taken as $x : y(1-x) : (1-y)(1-x)$, where x and y can be considered as the volume fractions of C in $C + Al_2O_3 + SiC$ and Al_2O_3 in $Al_2O_3 + SiC$, respectively. According to the rule of mixtures, the theoretical density, D, of each composition in the green state can be estimated from the following equation:

$$D = x \cdot D_C + y(1-x) \cdot D_{Al_2O_3} + (1-x)(1-y) \cdot D_{SiC} \quad (1)$$

where D_C, $D_{Al_2O_3}$ and D_{SiC} are the theoretical densities of C (2.26 g/cm^3), Al_2O_3 (3.96 g/cm^3) and SiC (3.22 g/cm^3), respectively.

The powder mixtures of C, Al_2O_3 and SiC were ball-milled in methanol for 24 h to increase the homogeneity. After drying in a rotary evaporator and sieving through a 60-mesh screen, the powders were uniaxially pressed into rectangular specimens of ~4.5 mm × 6.0 mm × 55 mm under a 50-MPa pressure using a stainless steel die. By a geometry method, the relative density of green compacts was examined to be ~60%, regardless of the differences in the volume fraction and particle size of graphite powders. Oxidation bonding was carried out in air using a one-step heating cycle in a box furnace with a heating and cooling rate of 5°C/min.

Weights of all individual specimens were measured before and after heat-treatment to estimate the oxidation degree of SiC particles in the OBSC process. Bulk density and open porosity were determined by the Archimedes method with distilled water as

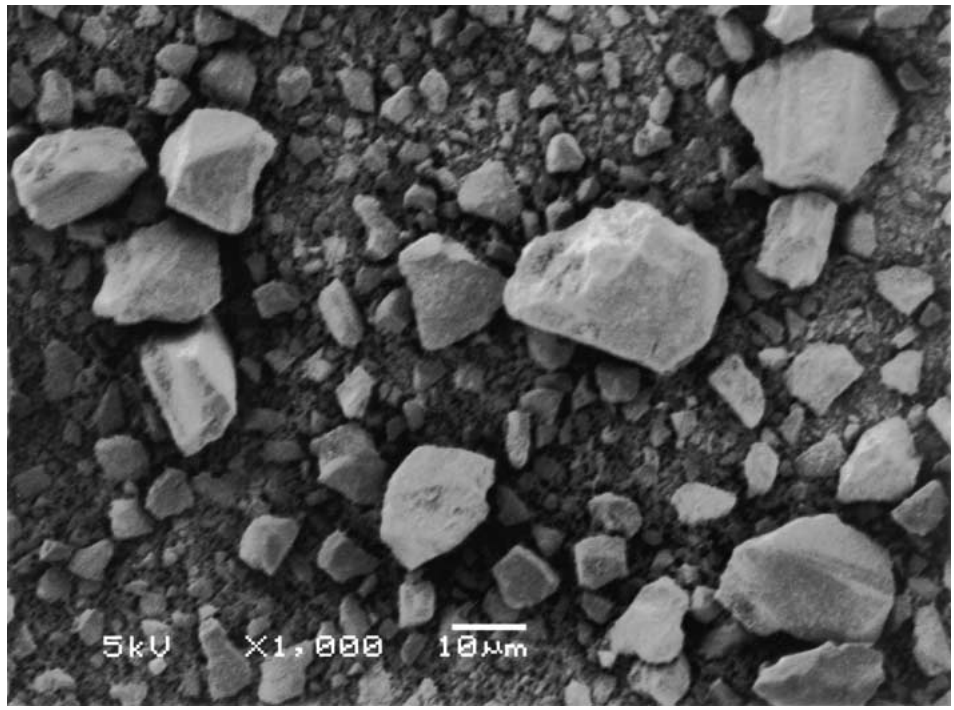

Figure 2 SEM micrograph of α-SiC powder.

the liquid medium. Phase analysis was conducted by X-ray diffraction (XRD) using a computer-controlled diffractometer (RINT2000, Rigaku Co., Tokyo, Japan) with Cu K_α radiation. Pore size distribution was determined by mercury porosimetry (Autopore 9220, Shimadzu Corp., Kyoto, Japan). Flexural strength was measured by a three-point bending test with a support distance of 30 mm and a cross-head speed of 0.5 mm/min on specimens of 3.0 mm $\times$ 4.0 mm $\times$ 40 mm. Four specimens were tested to obtain the average strength. Microstructures were observed by scanning electron microscopy (SEM). Moreover, the oxidation behaviors of SiC and C powders in air were evaluated by thermogravimetry (TG) analysis (Thermoplus TG 8120, Rigaku Co., Tokyo, Japan).

3. Results

To determine suitable heat-treatment conditions, a preliminary investigation was conducted on the powder compacts of $x = 0.25$ and $y = 0.15$ using a 5-μm-sized graphite powder. Since strength and porosity are two important parameters to be considered for a gas filter, they were evaluated as a function of heat-treatment temperature and time. It is obvious in Fig. 3 that the flexural strength increases and the open porosity decreases significantly with temperature from 1400° to 1450°C, but slightly with temperature from 1450° to 1500°C. When heat-treatment was performed at 1450°C, a notable increase in strength was achieved by increasing the holding time from 0.5 to 1 h. However, only a slight increase in strength was observed as the holding time was further extended to 2 h. Considering the fact that SiC oxidation may accelerate at higher temperatures and/or longer times, the processing temperature was fixed at 1450°C and the holding time was fixed to 1 h in the following experiments to investigate the effects of

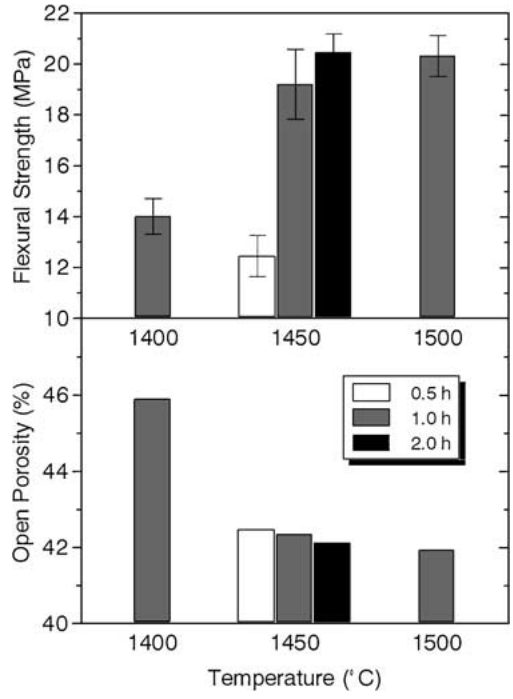

Figure 3 Flexural strength and open porosity as a function of processing temperature for a powder compact of $x = 0.25$ and $y = 0.15$, where a 5-μm-sized graphite powder was used.

Al_2O_3 additions as well as graphite particle size and volume fraction on oxidation degree, mechanical strength, open porosity and pore size distribution.

3.1. Effects of Al_2O_3 additions

The oxidation degree, open porosity and flexural strength of the OBSC specimens with different Al_2O_3 additions are summarized in Table I. When the volume fraction of Al_2O_3 addition increases from 0.05 to 0.25, the degree of SiC oxidation decreases slightly from 17.9 to 15.6%, but the open porosity decreases notably from

TABLE I Effect of Al_2O_3 additions on oxidation degree, open porosity and flexural strength for the OBSC specimens with $x = 0.25$

y	Oxidation degree (%)	Open porosity (%)	Flexural strength (MPa)
0.05	17.9	45.6	10.8 ± 1.2
0.15	16.9	42.4	19.2 ± 1.4
0.25	15.6	36.4	39.6 ± 1.9

TABLE II Effect of graphite particle size on oxidation degree, open porosity and flexural strength for the OBSC specimens with $x = y = 0.25$

C size (μm)	Oxidation degree (%)	Open porosity (%)	Flexural strength (MPa)
5	15.6	36.4	39.6 ± 1.9
10	15.5	39.9	32.0 ± 4.1
20	15.1	41.1	26.8 ± 5.9

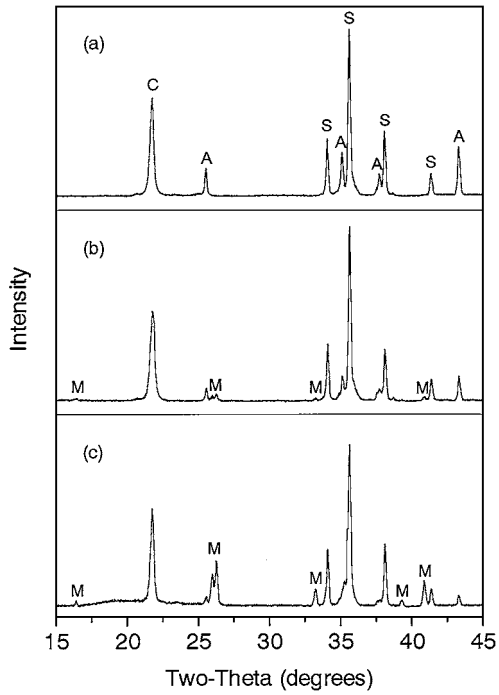

Figure 4 XRD patterns of the OBSC specimens with (a) $y = 0.05$, (b) $y = 0.15$ and (c) $y = 0.25$ (A is alumina, C is cristobalite, M is mullite, and S is silicon carbide).

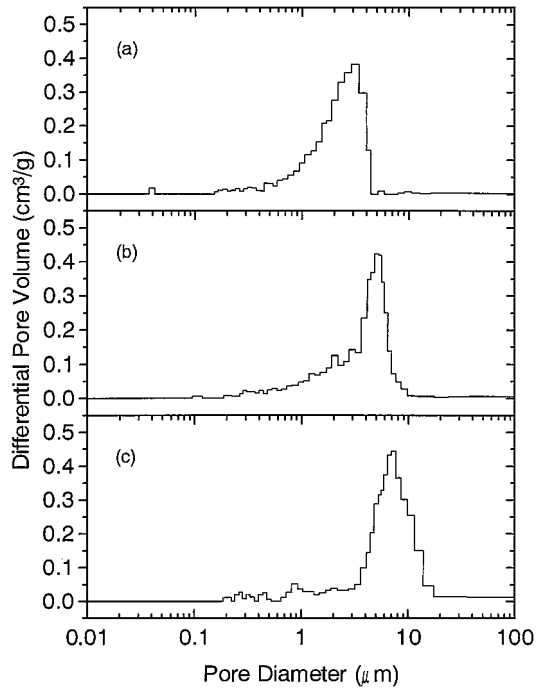

Figure 5 Pore size distribution in the OBSC specimens prepared using (a) 5-μm, (b) 10-μm and (c) 20-μm graphite particles.

45.6 to 36.4% and the flexural strength increases significantly from 10.8 to 39.6 MPa.

Fig. 4 shows the XRD patterns of the OBSC specimens with different Al_2O_3 additions. As shown, the OBSC specimens consist mostly of SiC, Al_2O_3 and cristobalite, but a small amount of mullite is also present due to the reaction between Al_2O_3 and SiO_2 at 1450°C. When more Al_2O_3 is added, the amount of mullite increases, as demonstrated in Fig. 4 by the increased intensity of the mullite peaks. On the other hand, the disappearance of the C peaks in the XRD patterns indicates that C has been completely burned out during heat-treatment.

3.2. Effects of graphite particle size

The effects of graphite particle size on the oxidation degree, open porosity and flexural strength of the OBSC specimens with $x = y = 0.25$ are shown in Table II. As expected, graphite particle size did not significantly affect on the degree of SiC oxidation. However, the open porosity increases and the flexural strength decreases with the increase in graphite particle size.

Further characterization of the pore size distribution in the OBSC specimens was performed using mercury porosimetry. As shown in Fig. 5, the pore size distribution is very broad in spite of the fact that graphite particles are quite homogenous. Moreover, the average pore diameter is much smaller than the added graphite particle size. For example, the average pore size is only $\sim$7.5 μm in the OBSC specimen prepared with 20-μm graphite particles. These "abnormal" phenomena will be discussed later.

3.3. Effects of graphite content

Table III lists the oxidation degree and open porosity of the OBSC specimens prepared with various graphite loadings. As can be seen, graphite content has little effect on the degree of SiC oxidation during heat-treatment. However, the open porosity is closely related to the level of graphite loading. When the graphite content increases from 25 to 60 vol%, the open porosity increases from 36.4 to 75.4%. This is consistent with the SEM observations that a relatively large amount of pores are present in the specimens with more graphite additions. Fig. 6 shows a typical microstructure of the

TABLE III Effect of graphite content on oxidation degree and open porosity for the OBSC specimens with $y = 0.25$

x	Oxidation degree (%)	Open porosity (%)
0.25	15.6	36.4
0.40	15.8	60.5
0.50	15.9	68.1
0.60	16.2	75.4

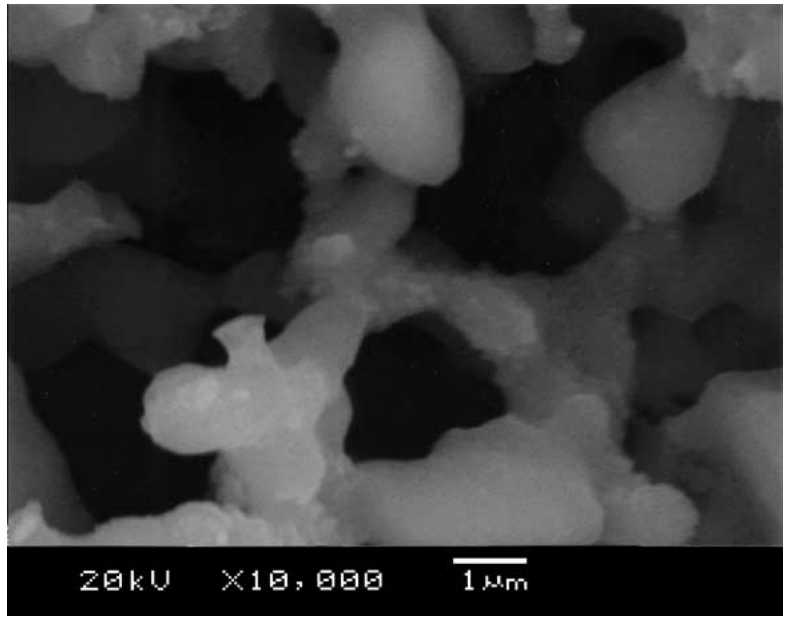

Figure 6 SEM micrograph of an OBSC specimen, which was prepared by adding 60 vol% of 5-μm-sized graphite particles.

OBSC specimen prepared with a 60 vol% graphite addition. Interestingly, the burnout of 60 vol% graphite did not destroy the structure of SiC particle networks. This suggests a potential advantage of the OBSC process for the fabrication of highly porous SiC ceramics.

4. Discussion

4.1. Oxidation behavior

It is known [14] that when identical spherical inclusions are randomly placed into a volume, at least one continuous network may percolate from one side of the volume to the other at an inclusion volume of ~16%. Another work [15] has shown that every inclusion is connected to the same percolating network at a volume of ≥22%. In the present work, the volume fraction of pores in the green compacts was ~40%. Thus, all the pores in the compacts should be connected each other, giving rise to an open porous network. It is more likely that such a connected network allows the diffusion of oxygen onto the surface of every SiC particle. This may account for the results in Tables II and III that the degree of SiC oxidation is almost independent of graphite particle size and volume fraction. However, the results in Table I indicate a slightly decreased oxidation degree for the specimen with more Al_2O_3 additions. This may be understood, because the surfaces of SiC particles can be partly covered by some fine Al_2O_3 powders, leading to the reduction in the surface area and thus in the oxidation degree.

Furthermore, a TG analysis was performed in air to determine the oxidation behaviors of SiC and C particles in the OBSC process. Since oxidation may cause a weight loss for C but a weight gain for SiC, it is evident in Fig. 7 that C oxidation begins at ~600°C and completes at ~900°C, while SiC starts to oxidize at ~750°C. This means that some graphite particles may remain in the structure and support the SiC networks before SiC oxidation. Once SiC begins to oxidize, the structure of the SiC particle network may be stabilized through the oxidation-derived SiO_2 glass, which bonds

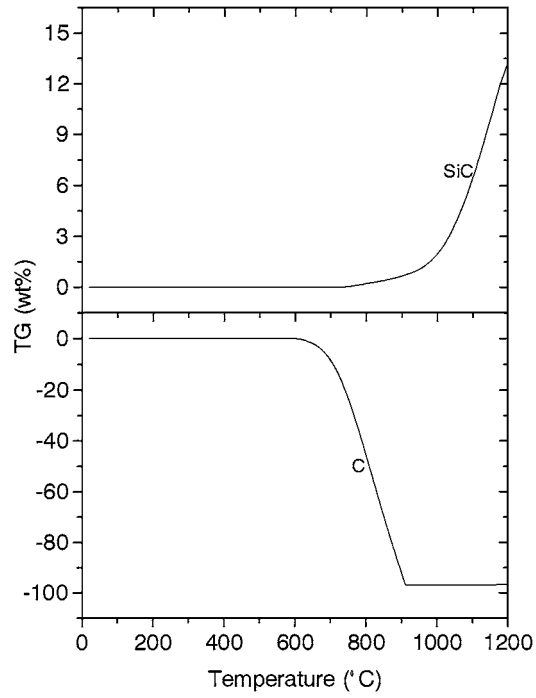

Figure 7 TG curves of the SiC and C powders heated in air at a rate of 5°C/min.

two neighboring SiC particles at the contacting points. Therefore, the OBSC process allows the preparation of porous SiC ceramics with a high porosity and a stable structure, as shown in Fig. 6. Such a highly porous structure cannot be achieved by a conventional sintering method, because the particle networks usually collapse when a large amount of pore-forming agent is removed [16].

Considering the fact that there is a layer of SiO_2 on the surface of every SiC particles, an excellent oxidation resistance is expected for the OBSC ceramics. To demonstrate this expectation, an OBSC specimen with $x = y = 0.25$ was oxidized in air at 1000°C for 50 h. After oxidation, the specimen exhibited a weight increase

of only ∼0.5%. This indicates that the OBSC ceramics are resistant to oxidation and thus suitable for some applications in oxidizing atmospheres.

4.2. Open porosity and pore size distribution

In the OBSC ceramics, all the pores can be considered as surface-connected open pores. Since the burnout of graphite particles leaves stable voids in the structure, the open porosity of the OBSC specimens increases almost linearly with the graphite content, as shown in Table III. On the other hand, larger graphite particles would result in larger voids, which may prevent the shrinkage of the structure and consequently cause an increased porosity. In contrast, more Al_2O_3 additions favor the shrinkage and therefore give a decreased porosity. These observations agree well with the experimental results in Tables II and III that the open porosity of the OBSC specimens increases with the graphite particle size but decreases with the Al_2O_3 content.

Usually, the size and distribution of graphite particles should be reflected in the pore-size distribution of the resultant porous microstructures, as demonstrated elsewhere [17–19]. However, the porosimetry results in Fig. 5 indicate that this is not the case. In fact, the data obtained by mercury porosimetry cannot reflect the real pore-size distribution, because such an analysis assumes pores with a cylindrical shape. In the present work, the pore channels were observed to have an irregular morphology. As shown in Fig. 8a, there is a narrow opening between two pores. Consequently, the measured pore sizes by mercury porosimetry should be the neck diameters between the pores. From the geometry shown schematically in Fig. 8b, the "pore" radium r_P can be easily derived as

$$r_P = \sqrt{r_{SiC}(r_{SiC} + 2r_C)} - r_{SiC} \quad (2)$$

where r_{SiC} and r_C are the particle radii of SiC and C, respectively. By taking r_{SiC} as 1.15 μm (the median radius of SiC particles), the average "pore" diameter, $2r_P$, was calculated to be 3.02, 4.86 and 7.56 μm for the OBSC specimens prepared with 5-, 10- and 20-μm graphite particles. This is in excellent agreement with the experimental results presented in Fig. 5. Also, the broad pore-size distribution in Fig. 5 should be a result of highly non-homogenous SiC particle size.

4.3. Flexural strength

The mechanical strength of porous ceramics depends strongly on porosity. To achieve a better understanding of the strength-porosity behavior for the porous OBSC ceramics, the porosity of the specimens with $x = y = 0.25$ was changed by varying the green density through the employment of different die-pressing pressures. The measured strengths are illustrated in Fig. 9 as a function of porosity. Evidently, the flexural strength decreases as the porosity increases. Generally, the strength-porosity dependence can be approximated by an exponential equation as follows [20–23]

$$\sigma = \sigma_0 \exp(-bP) \quad (3)$$

where σ_0 is the strength of a nonporous structure, σ is the strength of the porous structure at a porosity P, and b is an empirical constant. The fit of this equation to the results in Fig. 9 gave $\sigma_0 = 190$ MPa and $b = 4.36$, with a correlation factor $R^2 = 0.998$. Such a high R^2 value indicates that the strength-porosity behavior of the porous OBSC specimens can be well-described by the following equation

$$\sigma = 190 \exp(-4.36P) \quad (4)$$

However, it must be remembered that the values of $\sigma_0 = 190$ MPa and $b = 4.36$ would become different if the processing conditions and/or other parameters are changed. This can be demonstrated by comparing the

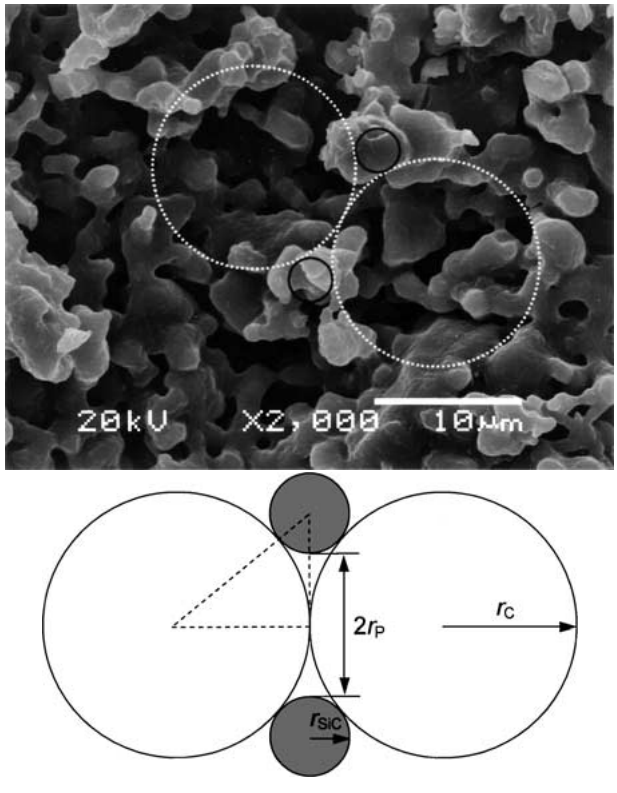

Figure 8 Structure of the pores in the OBSC ceramics: (a) SEM micrograph and (b) schematic diagram.

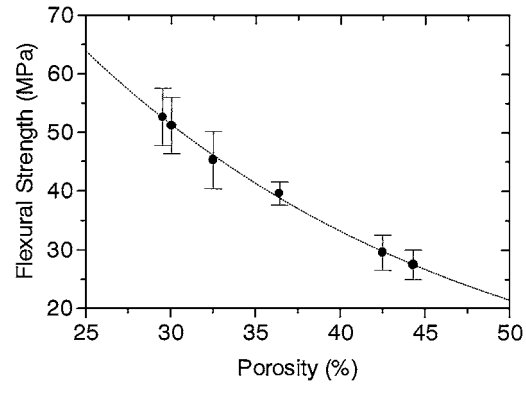

Figure 9 Strength as a function of porosity for the OBSC specimens with $x = y = 0.25$, where a 5-μm-sized graphite powder was used.

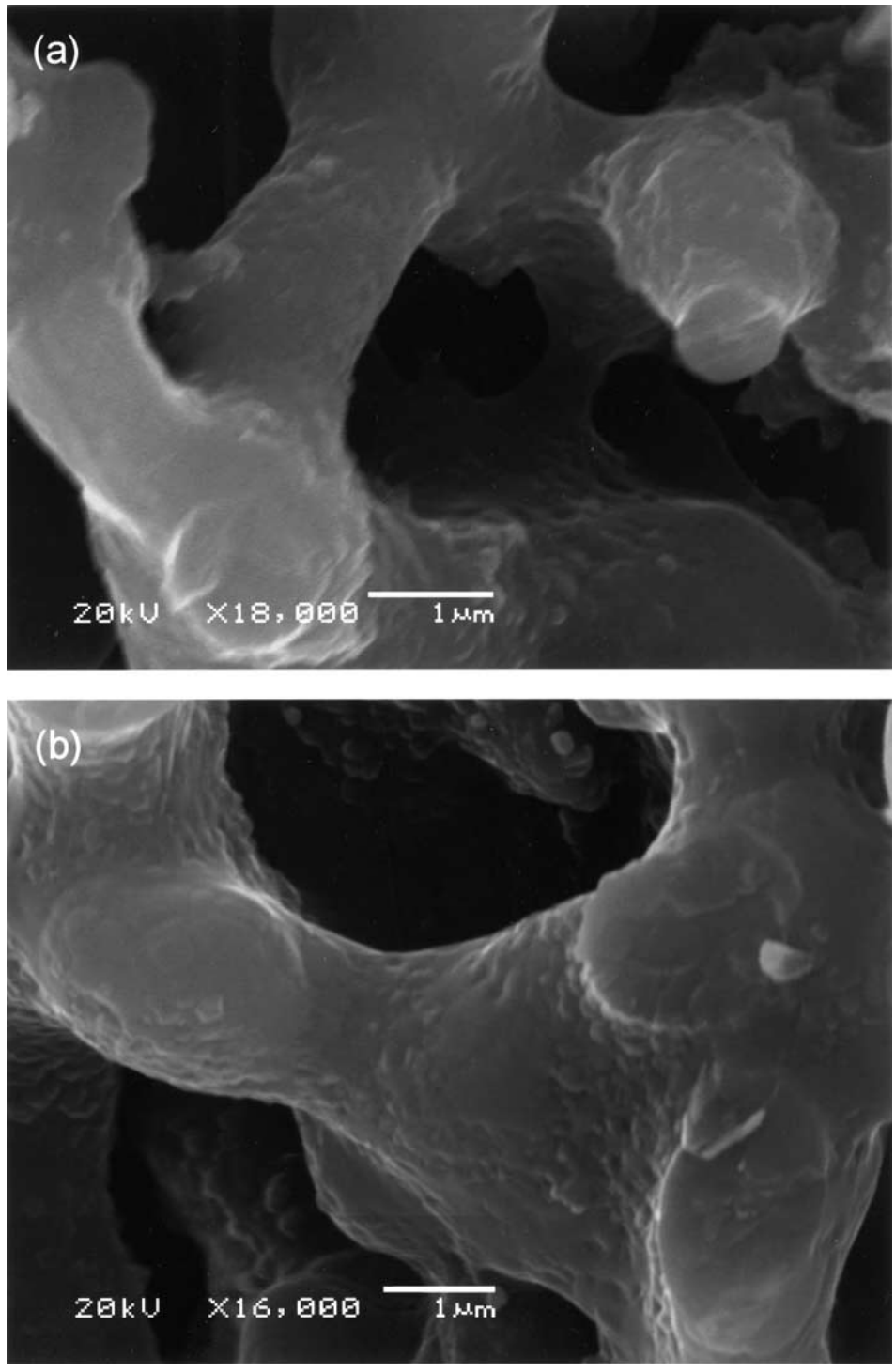

Figure 10 Fracture surfaces of the OBSC specimens with (a) $y = 0.05$ and (b) $y = 0.25$, where 25 vol% of 5-μm-sized graphite particles were added.

calculated and measured strengths of porous OBSC ceramics processed under different conditions. For example, the calculated strength was 31.7 MPa at $P = 41.1\%$. However, the result in Table II shows that the measured strength is only 26.8 MPa for the specimens prepared with 20-μm graphite particles. This indicates that the mechanical strength of the porous OBSC ceramics may be degraded by the increase in pore size. Recently, a similar phenomenon has been observed by Liu [24, 25] for porous hydroxyapatite bioceramics.

On the other hand, it is shown in Table I that the OBSC specimens with a porosity of 45.6% have an average strength of 10.8 MPa, which is much smaller than the calculated value of 26.0 MPa. This suggests that the strength of the porous OBSC ceramics may also be affected by other parameters except for porosity and pore size. It has been shown [20, 21, 26–30] that the fracture strength of porous ceramics is determined by the actual load-bearing area or the minimum solid area. In the present work, failure was observed to occur always at the necks between particles, as shown in Fig. 10. Therefore, the mechanical strength of the porous OBSC ceramics should also be related to the neck size. With less Al_2O_3 additions, the neck size is smaller (Fig. 10a), leading to a relatively low strength in comparison with the calculated value. When 25 vol% Al_2O_3 was added, the OBSC specimen with a porosity of 36.4% has a strength of 39.6 MPa, which is

much higher than the reported value of ~12 MPa for a commercially-available SCHUMALITH SiC at a similar porosity [31]. This should be mainly attributed to the well-developed necks, as shown in Fig. 10b.

In addition, it is interesting to note that the strength data of the porous OBSC ceramics are very uniform. For the specimens shown in Fig. 10b, the Weibull modulus was calculated to be as high as 21.5, regardless of the wide distribution in SiC particle sizes. This is not surprising, because the strength of the OBSC ceramics at a given porosity is determined mainly by the "oxide" necks rather than the SiC particle size.

5. Summary

Porous SiC ceramics were fabricated by a novel process referred to as oxidation bonding. In this process, the $SiC + Al_2O_3 + C$ powder compacts were heated in air rather than in an inert atmosphere. During heat-treatment, the graphite particles are burned out, leaving stable voids in the structure. At the same time, SiC particles could be bonded each other by the oxidation-derived SiO_2 glass. This allows the fabrication of porous SiC ceramics with a very high porosity. Another potential advantage of the present method is that the resultant SiC ceramics are highly resistant to oxidation, because there is a SiO_2 layer on the surface of every SiC particles. In addition, the pore structure can be easily controlled by the amount, size and distribution of graphite particles. Moreover, the oxidation-bonding technique is cost-effective as a result of low processing temperatures and inexpensive starting powders.

In this work, the effects of Al_2O_3 content as well as graphite particle size and volume fraction on the oxidation-bonding behavior, mechanical strength, open porosity and pore size distribution were investigated. It has been shown that the pore size and porosity depends strongly on graphite particle size and volume fraction. However, the degree of SiC oxidation was not observed to be significantly affected by graphite particle size and volume fraction. On the other hand, the mechanical strength of porous OBSC ceramics at a given porosity was found to be related to the sizes of pores and necks. In particular, the strength may be degraded by larger pores but enhanced by coarse necks. Due to the well-developed necks in the OBSC specimens with a 25 vol% Al_2O_3 addition, a high strength of 39.6 MPa was achieved at a porosity of 36.4%. Moreover, such a porous ceramic exhibited an excellent oxidation resistance and a high Weibull modulus. It is therefore anticipated that porous OBSC ceramics could be applicable for hot gas filtration in oxidizing atmospheres.

Acknowledgements

This work has been supported by METI as part of the Synergy Ceramics Project. The authors are members of the Joint Research Consortium of Synergy Ceramics. J. H. She would like to express his sincere thanks to JISTEC for an STA Fellowship.

References

1. L. MONTANARO, Y. JORAND, G. FANTOZZI and A. NEGRO, *J. Europ. Ceram. Soc.* **18** (1998) 1339.
2. J. M. TULLIANI, L. MONTANARO, T. J. BELL and V. SWAIN, *J. Amer. Ceram. Soc.* **82** (1999) 961.
3. K. SCHULZ, A. WALCH, E. FREUDE and M. DURST, in "High Temperature Gas Cleaning," edited by E. Schmidt, P. Gäng, T. Pilz and A. Dittler (Institut für Mechanische Verfahrenstechnik und Mechanik der Universität Karlsruhe, Karlsruhe, Germany, 1996) p. 835.
4. S. ITO, T. TANAKA and S. KAWAMURA, *Powder Technology* **100** (1998) 32.
5. M. A. ALVIN, *Materials at High Temperature* **14** (1997) 355.
6. *Idem.*, *Fuel Processing Technology* **56** (1998) 143.
7. R. WESTERHEIDE and J. ADLER, in "Ceramic Materials and Components for Engines," edited by J. G. Heinrich and F. Aldinger (Wiley-VCH Verlag, Weinheim, Germany, 2001) p. 73.
8. S. SCHEPPOKAT, R. JANSSEN and N. CLAUSSEN, *J. Amer. Ceram. Soc.* **82** (1999) 319.
9. P. MECHNICH, H. SCHNEIDER, M. SCHMÜCKER and B. SARUHAN, *ibid.* **81** (1998) 1931.
10. R. L. COBLE and W. D. KINGERY, *ibid.* **39** (1956) 377.
11. S. T. OH, K. I. TAJIMA, M. ANDO and T. OHJI, *ibid.* **83** (2000) 1314.
12. S. WU and N. CLAUSSEN, *ibid.* **74** (1991) 2460.
13. M. D. SACKS, K. WANG, G. W. SCHEIFFELE and N. BOZKURT, *ibid.* **80** (1997) 663.
14. F. ZOK, F. F. LANGE and J. R. PORTER, *ibid.* **74** (1991) 1880.
15. F. F. LANGE, L. ATTERAAS, F. ZOK and J. R. PORTER, *Acta Metall. Mater.* **39** (1991) 209.
16. Y. OHZAWA, T. SAKURAI and K. SUGIYAMA, *J. Mater. Processing Tech.* **96** (1999) 151.
17. S. F. CORBIN and P. S. APTE, *J. Amer. Ceram. Soc.* **82** (1999) 1693.
18. K. MACA, P. DOBSAK and A. R. BOCCACCINI, *Ceram. Int.* **27** (2001) 577.
19. S. F. CORBIN, J. LEE and X. QIAO, *J. Amer. Ceram. Soc.* **84** (2001) 41.
20. R. W. RICE, *J. Mater. Sci.* **28** (1993) 2187.
21. *Idem.*, in "Porosity of Ceramics" (Marcel Dekker, New York, 1998) p. 210.
22. K. ISHIZAKI, S. KOMARNENI and M. NANKO, in "Porous Materials: Process Technology and Applications" (Kluwer Academic Publishers, Dordrecht, The Netherlands, 1998) p. 202.
23. W. DUCKWORTH, *J. Amer. Ceram. Soc.* **36** (1953) 68.
24. D. M. LIU, *Ceram. Int.* **23** (1997) 135.
25. *Idem.*, *ibid.* **24** (1998) 441.
26. R. W. RICE, *J. Amer. Ceram. Soc.* **76** (1993) 1801.
27. *Idem.*, *Mater. Sci. Eng.* **A112** (1989) 215.
28. *Idem.*, *J. Mater. Sci.* **31** (1996) 1509.
29. A. HATTIANGADI and A. BANDYOPADHYAY, *J. Amer. Ceram. Soc.* **83** (2000) 2730.
30. Z. Y. DENG, T. FUKASAWA, M. ANDO, G. J. ZHANG and T. OHJI, *Acta Mater.* **49** (2001) 1939.
31. K. TANAKA, Y. AKINIWA, T. NOMURA and Y. SAKAIDA, *Trans. Jap. Soc. Mech. Eng.* **65** (1999) 2385.

Received 8 October 2001
and accepted 6 May 2002